

## Onset of Dendritic Flux Avalanches in Superconducting Films

D. V. Denisov,<sup>1,2</sup> D. V. Shantsev,<sup>1,2</sup> Y. M. Galperin,<sup>1,2</sup> Eun-Mi Choi,<sup>3</sup> Hyun-Sook Lee,<sup>3</sup> Sung-Ik Lee,<sup>3</sup> A. V. Bobyl,<sup>1,2</sup> P. E. Goa,<sup>1</sup> A. A. F. Olsen,<sup>1</sup> and T. H. Johansen<sup>1</sup>

<sup>1</sup>*Department of Physics and Center for Advanced Materials and Nanotechnology, University of Oslo, Post Office Box 1048 Blindern, 0316 Oslo, Norway*

<sup>2</sup>*A. F. Ioffe Physico-Technical Institute, Polytekhnicheskaya 26, St. Petersburg 194021, Russia*

<sup>3</sup>*National Creative Research Initiative Center for Superconductivity, Department of Physics, Pohang University of Science and Technology, Pohang 790-784, Korea*

(Received 5 April 2006; published 15 August 2006)

We report a detailed comparison of experimental data and theoretical predictions for the dendritic flux instability, believed to be a generic behavior of type-II superconducting films. It is shown that a thermomagnetic model published very recently [Phys. Rev. B **73**, 014512 (2006)] gives an excellent quantitative description of key features like the stability onset (first dendrite appearance) magnetic field, and how the onset field depends on both temperature and sample size. The measurements were made using magneto-optical imaging on a series of different strip-shaped samples of MgB<sub>2</sub>. Excellent agreement is also obtained by reanalyzing data previously published for Nb.

DOI: [10.1103/PhysRevLett.97.077002](https://doi.org/10.1103/PhysRevLett.97.077002)

PACS numbers: 74.25.Qt, 68.60.Dv, 74.25.Ha, 74.78.Db

Phenomena that create intriguing traces of activity that can be observed by direct visual methods are among the most fascinating things in nature. Penetration of magnetic flux in type-II superconductors seen by magneto-optical (MO) imaging is one example, where especially the spectacular dendritic flux patterns occurring in superconducting films are currently attracting much attention. The phenomenon has been observed in a large number of materials; YBa<sub>2</sub>Cu<sub>3</sub>O<sub>x</sub>, Nb, MgB<sub>2</sub>, Nb<sub>3</sub>Sn, NbN, YNi<sub>2</sub>B<sub>2</sub>C, and Pb [1–7], all films, and showing essentially the same characteristic behavior. In abrupt bursts the film becomes invaded by flux in narrow fingerlike regions that often form a complex and sample-spanning dendritic structure. These sudden events occur typically during a slow ramping of the applied magnetic field, and at temperatures below a certain fraction of the superconducting transition temperature,  $T_c$ . It is also characteristic that the flux patterns are never reproduced when experiments are repeated, see Fig. 1, thus ruling out possible explanations based on material defects guiding the flux motion. The massive experimental data existing today [1–15] indeed suggest that the phenomenon is a generic instability of the vortex matter in superconducting films. The emerging dendritic patterns are reminiscent of those formed during the crystal growth [16], viscous fluid flow [17], and electric discharge [18].

Abrupt flux avalanches are known to occur in superconductors for two fundamental reasons: (i) the motion of vortices releases energy, and hence increases the local temperature, and (ii) the temperature rise reduces flux pinning, and facilitates further vortex motion. This makes up a positive feedback loop that may lead to an instability [19,20]. However, why such avalanches should develop into dendritic patterns is a topic under vivid discussion, and several competing theories were recently proposed. They include a stability analysis taking into account the complex nonlocal electrostatics of thin film supercon-

ductors [21,22], a boundary layer model assuming shape-preserving fronts [23], and a shock wave approach [24], all leading to substantially different predictions. In this Letter we report on the first experiments designed specifically to check the validity of these models. It is shown that the model in Ref. [22] provides an excellent quantitative description of key features, such as the instability threshold field,  $H_{th}$ , i.e., the magnetic field when the first avalanche occurs, and how  $H_{th}$  depends on both temperature and the sample size. The results were obtained by MO imaging of flux penetration in MgB<sub>2</sub> films. Also earlier observations of Nb films [10] are shown to be in full agreement with this model.

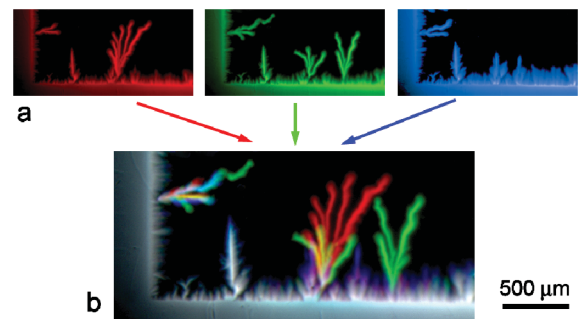


FIG. 1 (color). (a) Three MO images of flux penetration in MgB<sub>2</sub> taken during repeated identical experiments. (b) Image obtained by adding the 3 complementary colored images above. In the sum image the gray tone regions are those of repeated behavior, whereas colors show where there is no or only partial overlap. Strong irreproducibility is seen in the dendrite shapes, while the penetration near the edge and along static defects is reproducible. The dendrites tend to nucleate at preferred sites along the edge, which is due to small edge cavities giving local field amplification. The experiments were performed after cooling to 9.2 K and applying a magnetic field of 20 mT.

Thin films of  $\text{MgB}_2$  were fabricated by a two step process [25], where first a film of amorphous boron was deposited on an  $\text{Al}_2\text{O}_3$  (1 $\bar{1}$ 02) substrate using a pulsed laser. The B film and high-purity Mg were then put into a Nb tube, which was sealed in a high-purity Ar atmosphere and postannealed at 900 °C. To eliminate possible contamination with oxygen, water, and carbon, the samples were not exposed to air until the final form of the film was produced. The  $\text{MgB}_2$  films possess  $c$ -axis orientation, as confirmed by scanning electron microscopy, and magnetization data show a sharp superconducting transition at 39 K. The film thickness was 300 nm.

A set of eight  $\text{MgB}_2$  film samples was shaped by photolithography into 3 mm long rectangles having different widths ranging from 0.2 to 1.6 mm. All the samples were made from the same mother film, allowing simultaneous and comparative space-resolved magnetic observation [26]. An additional 5 mm wide sample was made using the same preparation conditions. A standard MO imaging setup with crossed polarizers and a ferrite garnet indicator was used to visualize flux distributions. Shown in Fig. 2 is

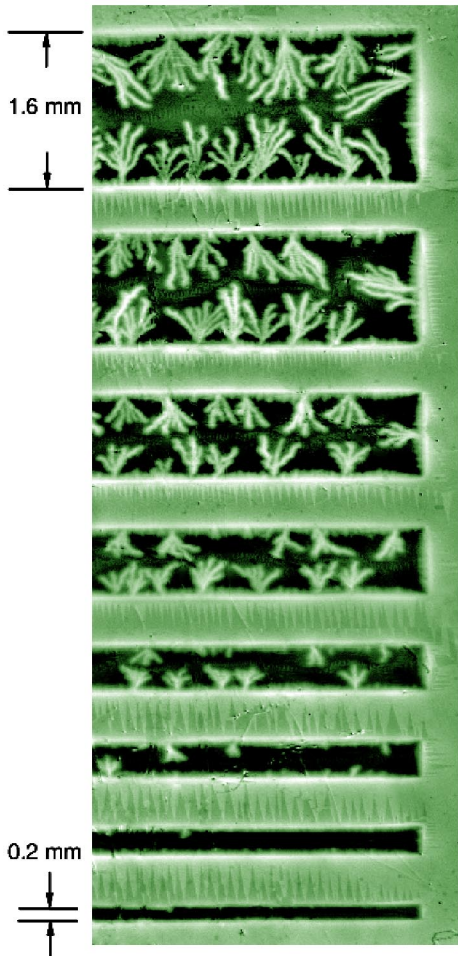


FIG. 2 (color online). MO image showing flux distribution in  $\text{MgB}_2$  strip-shaped samples at 4 K and 15 mT applied field. The image brightness represents the local flux density. Both the number and size of the dendrites are larger for the wider samples.

the flux penetration pattern when the eight samples, initially zero-field-cooled to 4 K, were exposed to a perpendicular applied magnetic field slowly ramped to 15 mT. The magnetic flux enters the superconductor in a form very much dominated by abrupt dendritic avalanches, although quite differently for the various samples. It is evident that the number of dendrites, their size, and branching habit depend strongly on the sample width. Whereas the wide strips become densely filled with flux dendrites, the more narrow samples contain fewer, until at the 0.2 mm wide strip flux dendrites almost never appear.

This qualitative result was followed up by measuring how the instability threshold field  $H_{\text{th}}$  depends on the strip width. Results obtained for all eight strips are shown in Fig. 3, where each data point represents an average over 4 repeated experiments using identical external conditions. The error bars indicate the scatter in the observed  $H_{\text{th}}$ . A variation as much as 30% implies that the nucleation of this instability is strongly affected by random processes, which is also consistent with earlier experiments [2,3,5,6,8,10]. Nevertheless, the data in Fig. 3 show a clear increase in the threshold field as the strip becomes narrower. In other words, reducing the sample width increases the stability of the superconductor.

Measurements of the temperature dependence of  $H_{\text{th}}$  are shown in Fig. 4. One sees that  $H_{\text{th}}$  not only increases with temperature, but appears to diverge at a certain temperature. Above this threshold temperature,  $T_{\text{th}}$ , found to be close to 10 K for  $\text{MgB}_2$  films, the dendritic instability disappears entirely. Included in the figure are also data we have extracted from a previous MO investigation of dendritic flux penetration in Nb films [10]. The two behaviors show remarkable similarities, although with different threshold temperatures, approximately 6 K in the Nb case.

To explain these observations we adopt the model developed in Refs. [21,22]. There, a linear analysis of the thermomagnetic instability in a long and thin superconducting strip thermally coupled to the substrate was worked out. The analysis considered a strip of width  $2w$

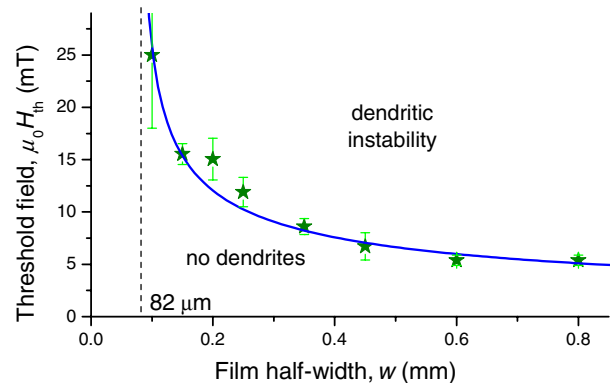


FIG. 3 (color online). Threshold magnetic field for onset of the dendritic instability in  $\text{MgB}_2$  strips of different width (symbols) plotted together with a fitted theoretical curve (full line), which diverges at a finite  $w$  indicated by the dashed asymptote.

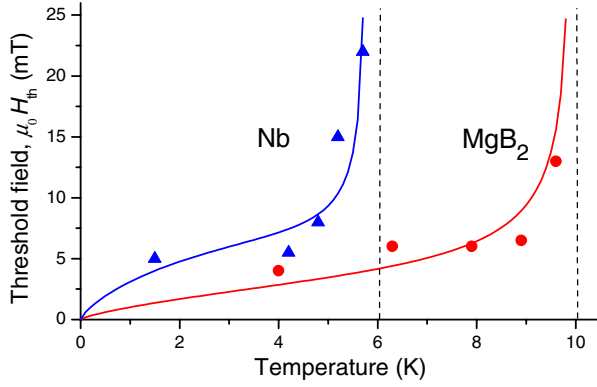


FIG. 4 (color online). Temperature dependence of the threshold magnetic field. Experimental data obtained for the 5 mm wide MgB<sub>2</sub> sample and for a 1.8 mm wide Nb film [10] are plotted as ● and ▲, respectively. The full lines are theoretical fits. The dashed lines show the limiting temperature above which the instability vanishes.

and thickness  $d \ll w$  placed in an increasing transverse magnetic field leading to a quasicritical state in the flux penetrated region near the edges. By solving the Maxwell and the thermal diffusion equations, it was shown that for small fields there are no solutions for perturbations growing in time, implying a stable situation. As the field increases the distribution can become unstable, with a fastest growing perturbation having a nonzero wave vector along the film edge. This means an instability will develop in the form of narrow fingers perpendicular to the edge—a scenario closely resembling the observed dendritic flux behavior. Within this model, the threshold flux penetration depth,  $l^*$ , when the superconducting strip first becomes unstable, is given by Eq. (25) of Ref. [22], which can be expressed as

$$l^* = \frac{\pi}{2} \sqrt{\frac{\kappa}{|j'_c|E}} \left(1 - \sqrt{\frac{2h_0}{nd|j'_c|E}}\right)^{-1}. \quad (1)$$

Here  $j'_c$  is the temperature derivative of the critical current density,  $\kappa$  is the thermal conductivity, and  $h_0$  is the coefficient of heat transfer from the superconducting film to the substrate. The parameter  $n \gg 1$  characterizes the strongly nonlinear current-voltage curve of the superconductor, described by the commonly used relation for the electrical field,  $E \propto j^n$ .

The threshold field,  $H_{th}$ , is obtained by combining Eq. (1) with the Bean model expression for the flux penetration depth of a long thin strip in a perpendicular applied field [27,28],

$$H_{th} = \frac{j_c d}{\pi} \operatorname{arccosh}\left(\frac{w}{w - l^*}\right). \quad (2)$$

Plotted in Fig. 3 as a solid line is this function using  $j_c = 9 \times 10^{10}$  A/m<sup>2</sup>, a value obtained for MgB<sub>2</sub> at 4 K by extrapolation of  $j_c(T)$  curves measured under the stable conditions above  $T_{th}$ . The only adjustable parameter,  $l^*$ ,

was chosen equal to 82  $\mu$ m, which gives an excellent agreement with our data. It follows from Eq. (2) that narrower strips need a larger field to reach the critical penetration depth  $l^*$ , which is exactly what we find experimentally. Furthermore, the model predicts that  $H_{th}$  should diverge when the strip half-width decreases towards  $w = l^*$ , this is also fully consistent with our MO observations.

To fit the observed  $H_{th}(T)$  one needs temperature dependent model parameters. We assume then a cubic dependence of the thermal conductivity,  $\kappa = \tilde{\kappa}(T/T_c)^3$ , as suggested by low-temperature data for MgB<sub>2</sub> [29]. Similarly, a cubic dependence of the heat transfer coefficient,  $h_0 = \tilde{h}_0(T/T_c)^3$  is chosen in accordance with the acoustic mismatch model confirmed experimentally for many solid-solid interfaces [30]. Furthermore, we assume a linear temperature dependence for the critical current density,  $j_c = j_{c0}(1 - T/T_c)$ , and with a pinning potential,  $U \propto 1 - T/T_c$ , the exponent  $n \sim U/kT$  also becomes  $T$  dependent,  $n = \tilde{n}(T_c/T - 1)$ .

Combining all these equations, one obtains a theoretical  $H_{th}(T)$ , and such curves fitted to experimental data for MgB<sub>2</sub> and Nb are shown in Fig. 4. MgB<sub>2</sub> data are presented for the largest (5 mm wide) film since here the instability is observed in the broadest temperature range. The model clearly reproduces the two key features; (i) the existence of a threshold temperature  $T_{th}$  above which the instability is absent, and (ii) a steep increase of the threshold field  $H_{th}$  when  $T$  approaches  $T_{th}$ . For MgB<sub>2</sub> the fit was made with  $j_{c0} = 10^{11}$  A/m<sup>2</sup>, and  $\tilde{\kappa} = 160$  W/K m [29], and choosing  $\tilde{n} = 10$  corresponding at  $T = 10$  K to the commonly used  $n = 30$ . The remaining parameters are the electric field and the heat transfer coefficient, where best fit was obtained with  $E = 30$  mV/m and  $\tilde{h}_0 = 17$  kW/K m<sup>2</sup>. It should be emphasized that the experimental data for both  $H_{th}(w)$  and  $H_{th}(T)$  were fitted using the same parameter values, and in both cases giving excellent quantitative agreement. Figure 4 also shows a similar fit for the data obtained for Nb, using  $T_c = 9.2$  K,  $j_{c0} = 10^{11}$  A/m<sup>2</sup>,  $w = 0.9$  mm,  $d = 0.5$   $\mu$ m, [10]  $\tilde{\kappa} = 120$  W/K m, [31]  $\tilde{n} = 40$ ,  $E = 200$  mV/m, and  $\tilde{h}_0 = 36$  kW/K m<sup>2</sup>. Again the model excellently describes the experimental behavior.

The fitted electric fields represent upper limiting values, since we used bulk values for thermal conductivity, which in general are larger than for films. Nevertheless, both values largely exceed the estimate,  $E \sim \dot{H}l^*$ , expected for a uniform and gradual flux penetration with a ramp rate of  $\dot{H} \approx 1$  mT/s as used in the experiments. We believe this discrepancy is due to the fact that local, rather than global, conditions govern the onset of the instability. Assuming that the flux dendrites are nucleated by abrupt microscopic avalanches of vortices [32], local short-lived electric fields can easily reach those high values. In fact, such avalanches consisting of  $10^2$ – $10^4$  vortices occurring in an area of  $\sim 20$   $\mu$ m were recently observed by high-resolution MO imaging in MgB<sub>2</sub> films [33]. Electric fields close to 30 mV/m would be created if such avalanches occur dur-

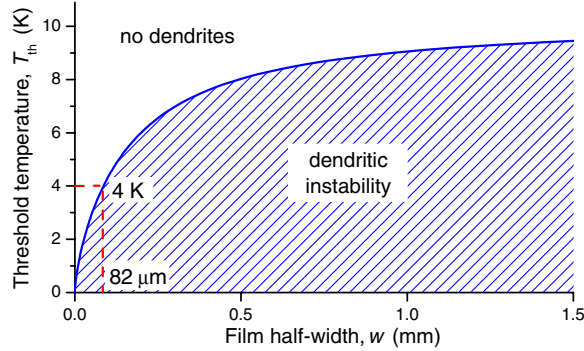


FIG. 5 (color online). Theoretical stability diagram predicting the threshold temperature  $T_{th}$  for different film width. The curve is plotted for parameter values corresponding to  $MgB_2$  films.

ing a time span of the order of  $10^{-5}$  s. Randomness in such avalanches may also explain the large scatter of the observed  $H_{th}$  values. We also note that the estimated electric field at the *nucleation* stage is still much lower than  $E$  values at the tip of an already *propagating* dendrite [34]. This fact is in agreement with expectations.

Finally, we emphasize that the two functions  $H_{th}(w)$  and  $H_{th}(T)$  have a similar feature, namely, a divergence at some value of the argument beyond which the system becomes stable, see Fig. 3 and 4. These stability thresholds are actually related to each other by the condition  $l^*(T_{th}) = w$ . The relation between the threshold temperature and the strip width is shown in Fig. 5, and represents the stability diagram in  $w - T$  coordinates, here plotted for parameters valid for  $MgB_2$ . It follows from the model that the temperature range of the instability increases monotonously with the strip width, but is limited upwards by a temperature close to 10 K for large-size films, as confirmed by many previous experiments [3,8,12–14]. The general result, that the instability is suppressed for sufficiently narrow strips, is of particular importance for design of superconducting electronic devices or other applications making use of thin film superconductors operating at temperatures below the instability threshold value.

This work is supported by the Norwegian Research Council, Grant No. 158518/431 (NANOMAT), by FUNMAT@UiO, and by the Ministry of Science and Technology of Korea through the Creative Research Initiative Program. We are thankful for helpful discussions with M. Welling and D. Lazuko.

- 
- [1] P. Leiderer *et al.*, Phys. Rev. Lett. **71**, 2646 (1993).
  - [2] C. A. Duran, P. L. Gammel, R. E. Miller, and D. J. Bishop, Phys. Rev. B **52**, 75 (1995).
  - [3] T. H. Johansen *et al.*, Supercond. Sci. Technol. **14**, 726 (2001).
  - [4] I. A. Rudnev *et al.*, Cryogenics **43**, 663 (2003).

- [5] I. A. Rudnev, D. V. Shantsev, T. H. Johansen, and A. E. Primenko, Appl. Phys. Lett. **87**, 042502 (2005).
- [6] S. C. Wimbush, B. Holzapfel, and Ch. Jooss, J. Appl. Phys. **96**, 3589 (2004).
- [7] M. Menghini *et al.*, Phys. Rev. B **71**, 104506 (2005).
- [8] T. H. Johansen *et al.*, Europhys. Lett. **59**, 599 (2002).
- [9] U. Bolz *et al.*, Europhys. Lett. **64**, 517 (2003).
- [10] M. S. Welling, R. J. Westerwaal, W. Lohstroh, and R. J. Wijngaarden, Physica (Amsterdam) **411C**, 11 (2004).
- [11] A. V. Bobyl *et al.*, Appl. Phys. Lett. **80**, 4588 (2002).
- [12] F. L. Barkov *et al.*, Phys. Rev. B **67**, 064513 (2003).
- [13] J. Albrecht *et al.*, Appl. Phys. Lett. **87**, 182501 (2005).
- [14] Zuxin Ye *et al.*, IEEE Trans. Appl. Supercond. **13**, 3722 (2003).
- [15] Eun-Mi Choi *et al.*, Appl. Phys. Lett. **87**, 152501 (2005).
- [16] J. S. Langer, Rev. Mod. Phys. **52**, 1 (1980).
- [17] P. G. Saffman and G. G. Taylor, Proc. R. Soc. A **245**, 312 (1958).
- [18] S. Pancheshnyi, M. Nudnova, and A. Starikovskii, Phys. Rev. E **71**, 016407 (2005).
- [19] R. G. Mints and A. L. Rakhmanov, Rev. Mod. Phys. **53**, 551 (1981).
- [20] S. L. Wipf, Cryogenics **31**, 936 (1991).
- [21] I. S. Aranson *et al.*, Phys. Rev. Lett. **94**, 037002 (2005).
- [22] D. V. Denisov, A. L. Rakhmanov, D. V. Shantsev, Y. M. Galperin, and T. H. Johansen, Phys. Rev. B **73**, 014512 (2006).
- [23] C. Baggio, R. E. Goldstein, A. I. Pesci, and W. van Saarloos, Phys. Rev. B **72**, 060503(R) (2005).
- [24] B. Rosenstein, B. Ya. Shapiro, and I. Shapiro, Europhys. Lett. **70**, 506 (2005).
- [25] W. N. Kang, Hyeong-Jin Kim, Eun-Mi Choi, C. U. Jung, and Sung-Ik Lee, Science **292**, 1521 (2001).
- [26] In principle, having several superconducting samples next to each other leads to crosstalk, i.e., a field expelled by one enhances the field experienced by another. This is a price to pay for being able to make direct comparative observations. Our distance between the strips was sufficiently large, as clearly seen from Fig. 2, where flux penetrates each strip equally from both sides. Had crosstalk been important, substantial asymmetry would be visible, especially in the upper sample having a neighbor only on one side.
- [27] E. Zeldov, J. R. Clem, M. McElfresh, and M. Darwin, Phys. Rev. B **49**, 9802 (1994).
- [28] E. H. Brandt and M. Indenbom, Phys. Rev. B **48**, 12 893 (1993).
- [29] M. Schneider *et al.*, Physica (Amsterdam) **363C**, 6 (2001).
- [30] E. T. Swartz and R. O. Pohl, Rev. Mod. Phys. **61**, 605 (1989).
- [31] F. Koechlin and B. Bonin, Supercond. Sci. Technol. **9**, 453 (1996).
- [32] E. Altshuler and T. H. Johansen, Rev. Mod. Phys. **76**, 471 (2004).
- [33] D. V. Shantsev, A. V. Bobyl, Y. M. Galperin, T. H. Johansen, and S. I. Lee, Phys. Rev. B **72**, 024541 (2005).
- [34] B. Biehler, B.-U. Runge, P. Leiderer, and R. G. Mints, Phys. Rev. B **72**, 024532 (2005).